The Astrophysical Journal, 846:73 (5pp), 2017 September 1 https://doi.org/10.3847/1538-4357/aa8669

ALMA Detects CO(3–2) within a Super Star Cluster in NGC 5253

Jean L. Turner[1], S. Michelle Consiglio[1], Sara C. Beck[2], W. M. Goss[3], Paul. T. P. Ho[4], David S. Meier[5], Sergiy Silich[6], and Jun-Hui Zhao[7]
[1] UCLA Department of Physics and Astronomy, Los Angeles, CA 90095-1547, USA; turner@astro.ucla.edu
[2] School of Physics and Astronomy, Tel Aviv University, Ramat Aviv, Israel
[3] National Radio Astronomy Observatory, Soccorro, NM 87801 USA
[4] Academia Sinica Astronomy and Astrophysics, Taipei, Taiwan
[5] Department of Physics, New Mexico Institute of Mining and Technology, Socorro, NM 87801 USA
[6] Instituto Nacional de Astrofísica, Óptica y Electrónica, Puebla, C. P. 72840, México
[7] Harvard-Smithsonian Center for Astrophysics, Cambridge, MA 02138 USA
Received 2017 June 15; revised 2017 July 28; accepted 2017 August 13; published 2017 September 1

Abstract

We present observations of CO(3–2) and ^{13}CO(3–2) emission near the supernebula in the dwarf galaxy NGC 5253, which contains one of the best examples of a potential globular cluster in formation. The 0.″3 resolution images reveal an unusual molecular cloud, "Cloud D1," that is coincident with the radio-infrared supernebula. The ∼6 pc diameter cloud has a linewidth, $\Delta v = 21.7$ km s^{-1}, that reflects only the gravitational potential of the star cluster residing within it. The corresponding virial mass is $2.5 \times 10^5\ M_\odot$. The cluster appears to have a top-heavy initial mass function, with $M_* \gtrsim$ 1–2 $M_\odot$. Cloud D1 is optically thin in CO(3–2), probably because the gas is hot. Molecular gas mass is very uncertain but constitutes <35% of the dynamical mass within the cloud boundaries. In spite of the presence of an estimated ∼1500–2000 O stars within the small cloud, the CO appears relatively undisturbed. We propose that Cloud D1 consists of molecular clumps or cores, possibly star-forming, orbiting with more evolved stars in the core of the giant cluster.

Key words: galaxies: star clusters: individual (NGC 5253 supernebula) – galaxies: star formation – H II regions – ISM: molecules

1. Introduction

Giant young star clusters, with masses $>10^5\ M_\odot$, contain thousands of massive stars within the space of only a few parsecs. Given the rapid rate of evolution of O stars, how other stars can form in their presence to build a large star cluster remains an outstanding problem. The closest young massive clusters are in nearby galaxies; at these distances, subarcsecond resolution is required to study star formation on cluster scales. The Atacama Large Millimeter/Submillimeter Array (ALMA) can now provide images of gas at subarcsecond resolution corresponding to cluster scales in local galaxies. The $J = 3$–2 line of CO is bright and easily excited in dense ($n \gtrsim 2 \times 10^4$ cm^{-3}) gas, and can be used to estimate gas masses and kinematics to study the star formation process and how feedback occurs within massive clusters.

NGC 5253 is a local (3.8 Mpc: $1'' = 18.4$ pc) dwarf spheroidal galaxy (Caldwell & Phillips 1989; Martin 1998) with many young star clusters (Caldwell & Phillips 1989; Meurer et al. 1995; Gorjian 1996; Calzetti et al. 1997; Tremonti et al. 2001; Harris et al. 2004; de Grijs et al. 2013; Calzetti et al. 2015) and an infrared luminosity of $\sim 10^9\ L_\odot$ (Vanzi & Sauvage 2004; Hunt et al. 2005). Its stellar mass is $\sim 2 \times 10^8\ M_\odot$ (Martin 1998, the dark matter mass could be ten times larger). At least one-third of the galaxy's infrared luminosity originates from a giant star-forming region, a compact ($\lesssim$3 pc) radio source known as the "supernebula" (Beck et al. 1996; Turner et al. 1998; Gorjian et al. 2001; Turner & Beck 2004; Rodríguez-Rico et al. 2007). Extinction toward the supernebula is high ($A_V \sim$ 16–18) (Calzetti et al. 1997; Turner et al. 2003; Martín-Hernández et al. 2005; Calzetti et al. 2015). The supernebula is coincident with a bright infrared source (Gorjian et al. 2001; Turner et al. 2003; Alonso-Herrero et al. 2004) that may coincide with a visible red cluster (i.e., #11) (Calzetti et al. 2015; Smith et al. 2016). Based on CO observations, there appears to be little molecular gas within NGC 5253; most of the CO emission is found in a streamer along the prominent minor axis dust lane (Turner et al. 1997; Meier et al. 2002; Miura et al. 2015). A bright CO(3–2) source was detected near the supernebula in 4″ observations with the Submillimeter Array; a comparison with lower J CO images suggests very warm gas, $T \gtrsim$ 200–300 K, in the central regions (Turner et al. 2015).

We present ALMA observations of CO and ^{13}CO $J = 3$–2 emission at ∼0.″3 resolution (5.5 pc) within the central region of NGC 5253. Requiring gas of density >20,000 cm^{-3} for collisional excitation, CO(3–2) traces the dense gas typically associated with star-forming cores (e.g., Myers 1985; Lada et al. 2010). The observations reveal a number of dense clouds within the central ∼100 pc starburst region identified as Cloud D by the CO(2-1) analysis of Meier et al. (2002); one cloud stands out in terms of its unusual properties. We present here an analysis of the coincidental molecular cloud coincident with the supernebula, henceforth denoted "Cloud D1."

2. Observations

NGC 5253 was observed in Band 7, which is a Cycle 1 program (ID = 2012.1.00105.S, PI = J. Turner) executed in Cycle 2 on 2015 June 4 and 5. The pointing shown here is centered at 13:39:44.911910, −31:38:26.49657 (J2000). The full mosaic of NGC 5253, including ^{13}CO(3–2), is presented elsewhere (Consiglio et al. 2017). Spectral windows have a total bandwidth of 937.500 MHz, with 244.141 kHz per channel. Velocities are barycentric, in radio convention. The bandpass and phase were calibrated with J1427-42064 and

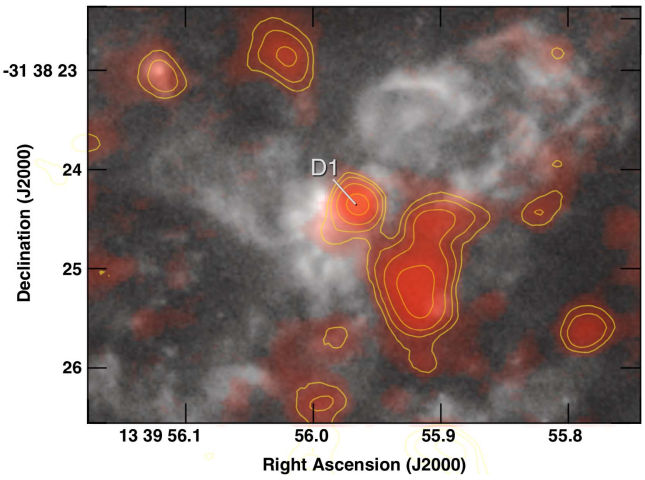

Figure 1. ALMA CO $J = 3$-2 emission in NGC 5253, in color and contours, superimposed on an archival *HST* Hα image. The ALMA beam is $0\farcs33 \times 0\farcs27$, p.a. $-90\fdg0$ (6 pc $\times$ 5 pc). The larger CO cloud to the southwest of D1 is ~15–20 pc away and redshifted with respect to D1. Cloud D1 is the focus of this paper; other clouds are discussed in Consiglio et al. (2017). For registration with the *HST* image, we assumed that D1, which is coincident with the radio continuum nebula, is coincident with the Pa β source in Calzetti et al. (2015).

J1342-2900, respectively. Titan was the flux calibrator. Calibration was done with CASA, pipeline 4.2.2 by the Joint ALMA Observatory. The absolute flux calibration is to within 10% for Cycle 2 Band 7 data (Lundgren 2013). Imaging was done with CASA pipeline 4.5.0 by the authors. The synthesized beam for the CO(3-2) maps is $0\farcs33 \times 0\farcs27$ p.a. $-90°$. The conversion to brightness is 1K ~9–17 mJy, with the smaller value for point sources, and the larger for sources filling the beam. A continuum map was constructed from offline channels in the band and subtracted from the (u, v) data by the authors before making line maps. The shortest baselines in the image are 25–100 kλ; emission more extended than ~4″ (~75 pc) can be poorly represented in these maps. From a comparison with SMA data, we estimate that ~50% of the emission is in such faint, extended structure (Consiglio et al. 2017). The rms noise in the individual 1 km s^{-1} line maps is 2.7 mJy/bm for CO(3-2) at 345.796 GHz. The integrated intensity map (Moment 0 map) was made by summing emission greater than $\pm 2.5\sigma$ in the cube.

3. Cloud D1 and the Supernebula

The ALMA image of CO(3-2) integrated line emission, in red and contours, is shown overlaid on an *Hubble Space Telescope* (*HST*) Hα image in Figure 1. At 10 times higher spatial resolution than previous CO maps, the ALMA CO(3–2) image reveals that what was previously identified as Cloud D (Meier et al. 2002; Turner et al. 2015) actually is composed of many molecular clouds. "Cloud D1," a compact and bright CO(3–2) source labeled in the figure, is coincident with the core of the radio/infrared supernebula. Fifteen to 20 parsecs to the southwest of D1 is a separate extended cloud with stronger CO(3–2) emission that is redshifted with respect to Cloud D1. There are numerous other clouds within the central region that are discussed elsewhere (Consiglio et al. 2017). In this paper, we focus on the unusual molecular Cloud D1.

NGC 5253 is a galaxy known for its bright nebular emission as well as for the presence of dust (Burbidge & Burbidge 1962; Kleinmann & Low 1970). The radio and mid-infrared emission in NGC 5253 is dominated by the supernebula, which is a source of radius <2 pc (Turner et al. 1998, 2000; Gorjian et al. 2001; Turner & Beck 2004) located near luminous and young star clusters (Meurer et al. 1995; Calzetti et al. 1997). From radio continuum fluxes (Turner et al. 1998, 2000; Meier et al. 2002; Turner & Beck 2004; Rodríguez-Rico et al. 2007), and radio recombination line fluxes (Rodríguez-Rico et al. 2007; Bendo et al. 2017), a Lyman continuum rate of $N_{\rm Lyc} \gtrsim 3.3 \times 10^{52}$ s^{-1} is indicated (corrected for direct dust absorption of ultraviolet (UV) photons following Inoue (2001), Turner et al. 2015). $N_{\rm Lyc}$ is computed for an ionization-bounded nebula and will be larger if there is photon leakage. Starburst99 models, described below, indicate that this Lyman continuum rate corresponds to ~1400–1800 O stars. The supernebula lies close to objects identified as Clusters 5 and 11 by Calzetti et al. (2015); from their colors, both appear to contain stars ~1 Myr in age (Calzetti et al. 2015; Smith et al. 2016).

Cloud D1 is located within 0.6 pc in projection of the embedded supernebula (Table 1; Turner & Beck 2004) The CO(3-2) line centroid, $v_{\rm bary} = 387.6 \pm 0.5$ km s^{-1}, agrees to <2 km s^{-1} with the main 10.5 μm [S IV] line from the ionized gas (Beck et al. 2012) and to <3 km s^{-1} with the H30α radio recombination line (Bendo et al. 2017) from the supernebula. Cloud D1 is thus coincident with the supernebula both in projection and in velocity, and it is similar if not identical in size.

Cloud D1 is small. A Gaussian fit to the integrated intensity image (Figure 1) gives a size of 220 ± 33 mas $\times$ 100 ± 54 mas, p.a. $2\fdg2 \pm 77°$, FWHM, deconvolved from the beam. Fits of D1 within the 24 individual channel maps within the FWHM give sizes of $\lesssim 0\farcs3 \pm 0\farcs05$. We adopt a size of

Table 1
Cloud D1 in NGC 5253

Quantity	Value
R.A.(2000)	$13^{\rm h}39^{\rm m}55\fs9561 \pm 0\fs0004$
Decl. (2000)	$-31°38'24\farcs364 \pm 0\farcs006$
Assumed distance	3.8 Mpc
V(CO(3-2))[a]	387.6 ± 0.5 km s^{-1}
ΔV(CO(3–2))[b]	21.7 ± 0.5 km s^{-1}
S(CO 3–2)[c]	2.2 ± 0.2 Jy km s^{-1}
S(^{13}CO3–2)[c]	0.05 ± 0.01 Jy km s^{-1}
Radius[d]	$0\farcs3 \pm 0\farcs05$
$M_{\rm vir}$[e]	$2.5 \pm 0.9 \times 10^5\ M_\odot$
$N_{\rm Lyc}$[f]	$3.3 \pm 0.3 \times 10^{52}$ s^{-1}

Notes.
[a] Line centroid, barycentric, and radio definition.
[b] FWHM; Gaussian fit to line in CASA.
[c] Integrated line fluxes are for 0.″5 aperture centered on D1. Uncertainty in the CO(3–2) flux is dominated by 10% calibration uncertainty; the ^{13}CO(3–2) flux uncertainty is due to signal to noise. See the text.
[d] Deconvolved from beam in CASA assuming a Gaussian source profile. See the text.
[e] Virial mass based on CO linewidth and size. For $\rho \propto 1/r$; for $1/r^2$ the mass is 30% less, and this is included in the uncertainty.
[f] Lyman continuum rate from the literature, primarily (Turner et al. 1998; Bendo et al. 2017), and is corrected for 30% direct absorption of UV photons by dust (Turner et al. 2015) following the procedure of Inoue (2001). Corrected to 3.8 Mpc. Assumes ionization-bounded nebula, and as such is a lower limit to the true rate.

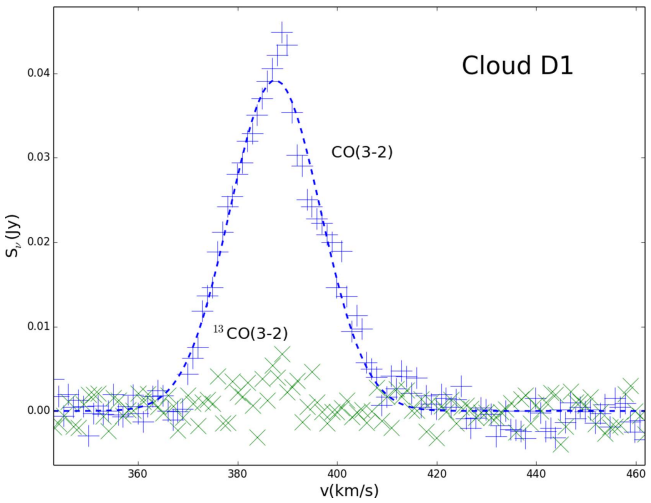

Figure 2. CO(3-2) (+) and ^{13}CO(3–2) (×) line profiles of Cloud D1 in NGC 5253. Fluxes in individual channels of the inner 0.″5 circular region centered on the CO(3-2) integrated intensity peak in Cloud D1 are plotted. Dashed curve is a least squares Gaussian fit to the CO(3–2) line. Channels are 1 km s^{-1}. The rms is 2.7 mJy, which is approximately the size of the crosses. Velocity is barycentric, radio convention.

0.″3 ± 0.″05, or $r = 2.8$ pc. Excitation of CO(3-2) requires minimum molecular gas densities of $n \gtrsim 20{,}000\,\mathrm{cm}^{-3}$, so the molecular gas in Cloud D1 is dense.

Cloud D1 is optically thin in the CO(3–2) line. In Figure 2, spectra are plotted for both CO(3-2) and ^{13}CO(3-2) lines within a 0.″5 region centered on Cloud D1. The integrated intensity of ^{12}CO(3–2) is $S_{CO} = 2.2 \pm 0.2$ Jy km s^{-1}; for ^{13}CO(3–2), it is $S_{13CO} \sim 40$–50 ± 8 mJy km s^{-1}. The line ratio of ∼50 for Cloud D1 is close to the abundance ratio of [CO]/[^{13}CO] ∼ 70 for the solar neighborhood, and the [C]/[^{13}C] ∼ 40–50 estimated for the Large Magellanic Cloud (LMC) (Heikkilä et al. 1999). The Cloud D1 ratio is significantly higher than the ∼11–15 observed in the nearby clouds, including the large cloud to the southwest of D1 (Consiglio et al. 2017), and is closer to the value of 13 observed in the Orion molecular cloud in optically thick, cool CO gas (Schilke et al. 1997). Warm gas can produce low optical depths in CO and this is what we propose for D1. For 300 K, as estimated from the modeling of the CO(3-2)/CO(1-0) line ratio (Turner et al. 2015), the CO partition function is ∼100, and the populations of the low J levels are correspondingly low. Thus, the low optical depth in the CO(3-2) line from Cloud D1 is additional evidence that the gas is in close proximity to the super star cluster.

A dynamical mass within Cloud D1 can be obtained from the width of the CO line, $\Delta v = 21.7 \pm 0.5$ km s^{-1} (FWHM). For an r^{-1} mass profile, as in the Galactic cloud W49N, $M_{\rm vir}(r < 2.8\,\mathrm{pc}) \sim 2.5 \pm 0.9 \times 10^5\,M_\odot$ (an r^{-2} profile would give ∼30% less mass). This mass estimate assumes a virialized cloud; it is unclear if this is valid for such a dynamic young source. However, most other sources of velocity (such as protostellar outflows or stellar winds) would, if anything, broaden the line over the gravitational value. Moreover, the mass is close to that expected from the star cluster based on its radio free–free flux. Hence, we adopt a gravitational mass of $2.5 \pm 0.9 \times 10^5\,M_\odot$. The mean mass density within the cloud region, most of which is in stars, is then 2700 $M_\odot$ pc^{-3}, corresponding to $\langle n_{\rm H2}\rangle \sim 40{,}000$ cm^{-3} and surface density $\Sigma_{D1} = 10^4\,M_\odot\,\mathrm{cm}^{-2} = 2.1\,\mathrm{g\,cm}^{-2}$, in the range observed for super star clusters (Tan et al. 2014). These would have been the original gas values at the onset of star formation in the cloud.

It is exceedingly difficult to determine a molecular gas mass for Cloud D1. The metallicity of the region is unclear. The galaxy overall is metal-poor, $Z \sim 0.25\,Z_\odot$, but there is evidence for localized enrichment near the young clusters (Walsh & Roy 1989; Schaerer et al. 1997; Kobulnicky et al. 1997; López-Sánchez et al. 2007; Turner et al. 2015). From the CO(3-2) line intensity of 2.2 ± 0.2 Jy km s^{-1}, and for $T_{ex} = 300$ K (an uncertain number; Turner et al. 2015), the mass in CO molecules alone is $M_{CO} = 3.0\,M_\odot$ for optically thin emission; then for a Galactic [CO]/[H$_2$], the molecular gas mass is $M_{\rm H2} \sim 3500\ M_\odot$ (this includes He; for $T = 50$ K, the mass would be ∼4 times lower.) However, the Galactic [CO]/[H$_2$] abundance may not be appropriate in this environment. An alternate method using an empirical CO "conversion factor," $X_{\rm CO} = 4.7 \times 10^{20}\,\mathrm{cm}^{-2}\,(\mathrm{K\,km/s}^{-1})^{-1}$, gives $M_{\rm gas} = 6.5 \times 10^4\,M_\odot$ (including He). Since this relation applies to gas-dominated, optically thick clouds, it should overestimate the gas mass in D1. The mass of ionized gas in the supernebula is $M_{\rm H\,II} \sim 2000\ M_\odot$ (Turner & Beck 2004); the estimated H I mass within D1 based on the 21 cm absorption column (Kobulnicky & Skillman 2008) toward the supernebula is minimal (∼200–500 $M_\odot$; larger H I columns will become molecular). The combined molecular-plus-ionized gas mass within Cloud D1 is $M_{\rm gas} \sim 6000$–$60{,}000\ M_\odot$. We estimate that gas constitutes <35% of the mass within the boundaries of Cloud D1.

Based on the dynamical mass from the CO linewidth, which is dominated by stars, we can compare the mass, $M_{\rm VIR}$, indicated for the cluster, and the observed Lyman continuum rate. We find $M_{\rm dyn}/L \lesssim 0.0005\ M_\odot/L_\odot$. We use Starburst99 models to model the cluster age and initial mass function (IMF). For the calculated $N_{\rm Lyc}$ and $M_{\rm dyn}$ (Table 1), Starburst99 (Leitherer et al. 1999, 2014) models were run for Padova and Geneva models for metallicities of Z = 0.004 (the closest to the mean metallicity of NGC 5253) and 0.008, with Kroupa IMFs with exponent 2.3. Statistical evidence (Weidner & Kroupa 2004; Oey & Clarke 2005; Kroupa et al. 2013) suggests an upper mass limit of ∼150 $M_\odot$ for stars. Starburst99 models with an upper IMF mass cutoff of 150 $M_\odot$ require a lower IMF mass cutoff $\gtrsim$2 $M_\odot$ to reach the observed $N_{\rm Lyc}$ for a cluster of $2 \times 10^5\ M_\odot$. It has been suggested that stars of 200 $M_\odot$ or more may exist in R136 and NGC 5253 (Crowther et al. 2010; Smith et al. 2016) and perhaps formed from binary mergers (Banerjee et al. 2012). Such supermassive stars could increase the Lyman continuum rate without adding much mass. Even for a 200 $M_\odot$ cutoff, Starburst99 models indicate a lower mass cutoff of $\gtrsim$1 $M_\odot$ for the D1 cluster. If there is leakage of UV photons beyond the supernebula, which would increase $N_{\rm Lyc}$, the lower mass cutoffs for the IMF are even higher. Another explanation for the low mass-to-luminosity ratio may be interacting binary stars (Stanway et al. 2016).

4. The Internal Structure of Cloud D1

Cloud D1 is located within the supernebula/cluster core, which is a harsh environment for molecules, where the mean separation between O stars is only ∼0.1 pc. The CO properties suggest that Cloud D1 is composed of many pockets of dense molecular gas, which may be in the form of protostellar disks, hot molecular cores surrounding individual stars, or residual dense molecular clumps. The estimated molecular gas mass of

$M_{H_2} = 3500$–$60{,}000\ M_\odot$, including He, predicts a column density of $N_{H_2} = 0.65$–11×10^{22} cm^{-2}, and a gas volume density of $M_{H2} = 570$–9800 cm^{-3}. A comparison with the CO(3–2) critical density of $\gtrsim$20000 cm^{-3} indicates a volume filling factor of $\lesssim$3%–50%. We regard the lower value, corresponding to the optically thin mass, as more likely, and a the volume filling factor of $f_{vol} \lesssim 10\%$.

The smooth and near-Gaussian CO line profile and the similarity in shape of D1 across the line also suggests many clumps. Figure 2 shows the CO(3–2) line profile and the Gaussian fit. Departures from smoothness can be used to estimate numbers of clumps, even if the line is not perfectly Gaussian (Beck 2008). Channel-to-channel variations for the central 24 channels are typically $\lesssim$20%, implying $\sim$25 clumps per channel and $N_{cl} \gtrsim 600$ for clumps with individual thermal linewidths of $\sim$1 km s^{-1}. If instead Cloud D1 is composed of CO protostellar disks or molecular cores surrounding individual stars, with expected linewidths of 1–10 km s^{-1}, then fewer disks/cores are needed to produce a smooth line. Spatial variations in the centroid and deconvolved size of the emission from Cloud D1 across the 24 line channels are also consistent with no variation (centroids coincident to $\lesssim$20 mas and in size, to $\lesssim$50 mas), consistent with the many-clump hypothesis. The slight nonGaussianity would be consistent with randomly distributed substructures. The blueshifted side of the line is smoother than the redshifted side, which has no clear explanation; the redshifted side may be related to the southeastern extension of the cloud.

Are these small clumps or cores consistent with the radiation shielding necessary for the existence of CO? There is a minimum size expected for CO-emitting clouds, since CO is chemically sustained only at $A_v > 2$ or cloud column $A_v > 4$ (Hollenbach & Tielens 1999; Bisbas et al. 2015). At a density of $n_{crit} = 30{,}000$ cm^{-3} (for $T = 300$K), the minimum cloud column corresponds to a distance of 0.04 pc = 8000 au for a Galactic $A_V/(N_H + 2N_{H2})$ ratio. The corresponding minimum clump mass is 0.1 $M_\odot$. It is thus plausible that Cloud D1 could accommodate these minimum A_v clumps both in linear dimension and in mass.

5. Feedback and Star Formation within a Young, Massive Cluster

Cloud D1 coincides with the supernebula, which is an ultracompact H II region, and nearby evidence of Wolf–Rayet stars (Walsh & Roy 1989; Kobulnicky et al. 1997; Schaerer et al. 1997; López-Sánchez et al. 2007) that are typically 3–4 Myr in age, but sometimes less (Smith et al. 2016). Wolf–Rayet stars can lose copious amounts of metal-enriched mass. Thus, the presence of molecular gas may not in itself give a good indication of cluster age. Some super star clusters appear to be actively dispersing gas in winds, as appears to be occurring in NGC 253 (Sakamoto et al. 2006; Bolatto et al. 2013). However, if the cluster is sufficiently massive, theory suggests that the evolution of the H II region can be affected by gravity (Kroupa & Boily 2002; Murray et al. 2010), so that in some cases the enriched products of stellar mass loss may be retained by the cluster (Silich & Tenorio-Tagle 2017). Cloud D1 could perhaps survive after a supernova, since simulations suggest that gas can backfill into the cluster after the explosion (Tenorio-Tagle et al. 2015). We note that the CO linewidth reflecting the core cluster mass within the supernebula is almost precisely equal to the thermal linewidth of the ionized hydrogen; this may not be coincidence.

To put Cloud D1 in perspective, it is instructive to compare it with its closest Galactic analog, W49N. Of similar extent ($r \sim 3$ pc) with ultracompact H II regions (Dreher et al. 1984; De Pree et al. 2000), W49N appears to be at a similar evolutionary stage to the supernebula in NGC 5253. W49N has a luminosity of $7 \times 10^6\ L_\odot$(Buckley & Ward-Thompson 1996), which is 100 times less that of the supernebula. Yet W49N has a larger, perhaps significantly larger, molecular gas mass, $\sim 1.2 \times 10^5\ M_\odot$ (Galván-Madrid et al. 2013). Even including the cloud to the southwest of the supernebula that is of a similar mass to the W49N cloud (Consiglio et al. 2017), the supernebula region is $\sim$50 times more efficient than W49N at forming stars in terms of L_{IR}/M_{H2}.

An alternative to high star formation efficiency is that gas has already dispersed from the young cluster. Based on the CO linewidth, the dispersal of gas from the cluster does not appear to be occurring at present. Given the young age of the cluster, any gas that has previously been dispersed by the cluster cannot be far away. Gas expelled at $\sim$20 km s^{-1}, the overall velocity dispersion within the region (Consiglio et al. 2017), would still be within $\sim$20–60 pc of the cluster given its age; the clouds will still lie within Figure 1.

The continued presence of dense molecular gas within the supernebula cluster and its relative quiescence suggests that negative star formation feedback effects are minimal on the molecular gas at this stage of cluster evolution of the supernebula, perhaps because the gas is in the form of compact clumps or cores. The high density indicated by the CO(3–2) emission suggests that Cloud D1 may still be forming stars. The CO(3-2) emission may arise in dense hot molecular cores around young stellar objects, which would be consistent with the warm, $T_K \gtrsim 300$K temperature suggested by lower resolution CO line ratios (Turner et al. 2015), and the optically thin CO(3–2) emission reported here. For this temperature, and given that the CO cores are embedded in an H II region of density $n_H = 3.5 \times 10^4$ cm^{-3} (Turner & Beck 2004), the Bonnor–Ebert mass of Cloud D1 is $M_{BE} \sim 13\ M_\odot$. If stars are still forming within the core of the cluster embedded in Cloud D1, they will be massive.

6. Conclusions

We present ALMA observations of CO(3–2) and ^{13}CO(3–2) at 0.″3 resolution of the region surrounding the supernebula in NGC 5253. We identify an unusual cloud, "Cloud D1," that is precisely coincident with the supernebula/ embedded cluster in space and velocity. Cloud D1 has a radius of $r \sim 2.8$ pc, nearly the same size as the supernebula. Based on

(1) spatial coincidence to <0.6 pc in projection with the supernebula,
(2) velocity coincidence to within 2–3 km s^{-1} with mid-IR nebular and radio recombination lines from the H II region, and
(3) the fact that the cloud is optically thin, probably because it is hot,

we conclude that the molecular cloud is mixed in with the super star cluster, which contains $\sim$1500 O stars, and the compact H II region.

The CO linewidth of 21.7 km s^{-1} indicates that the CO gas in Cloud D1 is relatively undisturbed in spite of its location within

this dense cluster. The linewidth indicates a dynamical mass of $M_{\rm dyn} = 2.5 \times 10^5\ M_\odot$. This gives $M/L \sim 5 \times 10^{-4}\ M_\odot/L_\odot$ for the cluster, implying a top-heavy IMF, with lower cutoff of $\gtrsim$1–2 $M_\odot$, and more if there is photon leakage beyond the supernebula.

A CO(3–2)/^{13}CO ratio of ∼50 indicates the the emission from Cloud D1 is bright because the gas is optically thin and warm. Estimates of gas mass based on this line are uncertain, but suggest that the molecular gas mass is <60,000 $M_\odot$. The star formation efficiency appears to be $\gtrsim$50 times that of W49N, the closest Galactic analog. The smoothness of the CO line profile and its near Gaussianity suggests Cloud D1 consists of many, up to hundreds, of molecular clumps or cores. Given the high ambient pressure and temperature within Cloud D1, if the cloud is indeed hot as previously estimated (Turner et al. 2015) only massive stars $\gtrsim$13 $M_\odot$ can form at present. We propose that Cloud D1 is composed of many hot molecular clumps or cores orbiting within the cluster potential with the stars of the super star cluster and may yet be capable of forming stars.

This paper makes use of the following ALMA data: ADS/JAO.ALMA# 2012.1.00125.S. ALMA is a partnership of ESO (representing its member states), NSF (USA), and NINS (Japan), together with NRC (Canada) and NSC and ASIAA (Taiwan), in cooperation with the Republic of Chile. The Joint ALMA Observatory is operated by ESO, AUI/NRAO, and NAOJ. The National Radio Astronomy Observatory is a facility of the National Science Foundation (NSF) operated under cooperative agreement by Associated Universities, Inc. S.M.C. acknowledges the support of an NRAO Student Observing Support Grant. The authors thank Adam Ginsburg, Christian Henkel, Leslie Hunt, Pavel Kroupa, Phil Myers, Nick Scoville, and an anonymous referee for helpful discussions and comments. J.L.T. acknowledges additional support from NSF grant AST 1515570, and from a COR grant from the UCLA Academic Senate.

Facility: ALMA.

Software: Starburst99 (Leitherer et al. 1999), CASA, AIPS, SAOImage DS9.

ORCID iDs

Jean L. Turner https://orcid.org/0000-0003-4625-2951
S. Michelle Consiglio https://orcid.org/0000-0002-0214-0491
David S. Meier https://orcid.org/0000-0001-9436-9471
Sergiy Silich https://orcid.org/0000-0002-3814-5294
Jun-Hui Zhao https://orcid.org/0000-0002-1317-3328

References

Alonso-Herrero, A., Takagi, T., Baker, A. J., et al. 2004, ApJ, 612, 222
Banerjee, S., Kroupa, P., & Oh, S. 2012, MNRAS, 426, 1416
Beck, S. C. 2008, A&A, 489, 567
Beck, S. C., Lacy, J. H., Turner, J. L., et al. 2012, ApJ, 755, 59
Beck, S. C., Turner, J. L., Ho, P. T. P., Lacy, J. H., & Kelly, D. M. 1996, ApJ, 457, 610
Bendo, G. J., Miura, R. E., Espada, D., et al. 2017, MNRAS, in press (arXiv:1707.06184)
Bisbas, T. G., Haworth, T. J., Barlow, M. J., et al. 2015, MNRAS, 454, 2828
Bolatto, A. D., Warren, S. R., Leroy, A. K., et al. 2013, Natur, 499, 450
Buckley, H. D., & Ward-Thompson, D. 1996, MNRAS, 281, 294
Burbidge, E. M., & Burbidge, G. R. 1962, ApJ, 135, 694
Caldwell, N., & Phillips, M. M. 1989, ApJ, 338, 789
Calzetti, D., Johnson, K. E., Adamo, A., et al. 2015, ApJ, 811, 75
Calzetti, D., Meurer, G. R., Bohlin, R. C., et al. 1997, AJ, 114, 1834
Consiglio, S. M., Turner, J. L., Beck, S. C., et al. 2017, ApJ, submitted (arXiv:1706.09944)
Cresci, G., Vanzi, L., & Sauvage, M. 2005, A&A, 433, 447
Crowther, P. A., Schnurr, O., Hirschi, R., et al. 2010, MNRAS, 408, 731
de Grijs, R., Anders, P., Zackrisson, E., & Östlin, G. 2013, MNRAS, 431, 2917
De Pree, C. G., Wilner, D. J., Goss, W. M., Welch, W. J., & McGrath, E. 2000, ApJ, 540, 308
Dreher, J. W., Johnston, K. J., Welch, W. J., & Walker, R. C. 1984, ApJ, 283, 632
Galván-Madrid, R., Liu, H. B., Zhang, Z.-Y., et al. 2013, ApJ, 779, 121
Gorjian, V. 1996, AJ, 112, 1886
Gorjian, V., Turner, J. L., & Beck, S. C. 2001, ApJL, 554, L29
Harris, J., Calzetti, D., Gallagher, J. S., III, Smith, D. A., & Conselice, C. J. 2004, ApJ, 603, 503
Heikkilä, A., Johansson, L. E. B., & Olofsson, H. 1999, A&A, 344, 817
Hollenbach, D. J., & Tielens, A. G. G. M. 1999, RvMP, 71, 173
Hunt, L., Bianchi, S., & Maiolino, R. 2005, A&A, 434, 849
Inoue, A. K. 2001, AJ, 122, 1788
Kleinmann, D. E., & Low, F. J. 1970, ApJL, 159, L165
Kobulnicky, H. A., & Skillman, E. D. 2008, AJ, 135, 527
Kobulnicky, H. A., Skillman, E. D., Roy, J.-R., Walsh, J. R., & Rosa, M. R. 1997, ApJ, 477, 679
Kroupa, P., & Boily, C. M. 2002, MNRAS, 336, 1188
Kroupa, P., Weidner, C., Pflamm-Altenburg, J., et al. 2013, in Planets, Stars and Stellar Systems: Galactic Structure and Stellar Populations, Vol. 5, ed. T. D. Oswalt & G. Gilmore (Dordrecht: Springer), 115
Lada, C. J., Lombardi, M., & Alves, J. F. 2010, ApJ, 724, 687
Leitherer, C., Ekström, S., Meynet, G., et al. 2014, ApJS, 212, 14
Leitherer, C., Schaerer, D., Goldader, J. D., et al. 1999, ApJS, 123, 3
López-Sánchez, Á. R., Esteban, C., García-Rojas, J., Peimbert, M., & Rodríguez, M. 2007, ApJ, 656, 168
Lundgren, A. 2013, ALMA Cycle 2 Technical Handbook Version 1.1, ALMA
Martin, C. L. 1998, ApJ, 506, 222
Martín-Hernández, N. L., Schaerer, D., & Sauvage, M. 2005, A&A, 429, 449
Meier, D. S., Turner, J. L., & Beck, S. C. 2002, AJ, 124, 877
Meurer, G. R., Heckman, T. M., Leitherer, C., et al. 1995, AJ, 110, 2665
Miura, R. E., Espada, D., Sugai, H., Nakanishi, K., & Hirota, A. 2015, PASJ, 67, L1
Murray, N., Quataert, E., & Thompson, T. A. 2010, ApJ, 709, 191
Myers, P. C. 1985, in Protostars and Planets II, ed. D. C. Black & M. S. Matthews (Tucson, AZ: Univ. of Arizona Press), 81
Oey, M. S., & Clarke, C. J. 2005, ApJL, 620, L43
Rodríguez-Rico, C. A., Goss, W. M., Turner, J. L., & Gómez, Y. 2007, ApJ, 670, 295
Sakamoto, K., Ho, P. T. P., Iono, D., et al. 2006, ApJ, 636, 685
Schaerer, D., Contini, T., Kunth, D., & Meynet, G. 1997, ApJL, 481, L75
Schilke, P., Groesbeck, T. D., Blake, G. A., & Phillips, T. G. 1997, ApJS, 108, 301
Silich, S., & Tenorio-Tagle, G. 2017, MNRAS, 465, 1375
Smith, L. J., Crowther, P. A., Calzetti, D., & Sidoli, F. 2016, ApJ, 823, 38
Stanway, E. R., Eldridge, J. J., & Becker, G. D. 2016, MNRAS, 456, 485
Tan, J. C., Beltrán, M. T., Caselli, P., et al. 2014, in Protostars and Planets VI, ed. H. Beuther et al. (Tucson, AZ: Univ. of Arizona Press), 149
Tenorio-Tagle, G., Muñoz-Tuñón, C., Silich, S., & Cassisi, S. 2015, ApJL, 814, L8
Tremonti, C. A., Calzetti, D., Leitherer, C., & Heckman, T. M. 2001, ApJ, 555, 322
Turner, J. L., & Beck, S. C. 2004, ApJL, 602, L85
Turner, J. L., Beck, S. C., Benford, D. J., et al. 2015, Natur, 519, 7543
Turner, J. L., Beck, S. C., Crosthwaite, L. P., et al. 2003, Natur, 423, 621
Turner, J. L., Beck, S. C., & Ho, P. T. P. 2000, ApJL, 532, L109
Turner, J. L., Beck, S. C., & Hurt, R. L. 1997, ApJL, 474, L11
Turner, J. L., Ho, P. T. P., & Beck, S. C. 1998, AJ, 116, 1212
Vanzi, L., & Sauvage, M. 2004, A&A, 415, 509
Walsh, J. R., & Roy, J.-R. 1989, MNRAS, 239, 297
Weidner, C., & Kroupa, P. 2004, MNRAS, 348, 187